

EXPLORING GRAVITATION IN THE INNER SOLAR SYSTEM: GIUSEPPE COLOMBO, MERCURY AND THE BEPICOLOMBO MISSION

ROBERTO PERON

ISTITUTO DI ASTROFISICA E PLANETOLOGIA SPAZIALI (IAPS-INAf)

ROBERTO.PERON@INAF.IT

BEPICOLOMBO

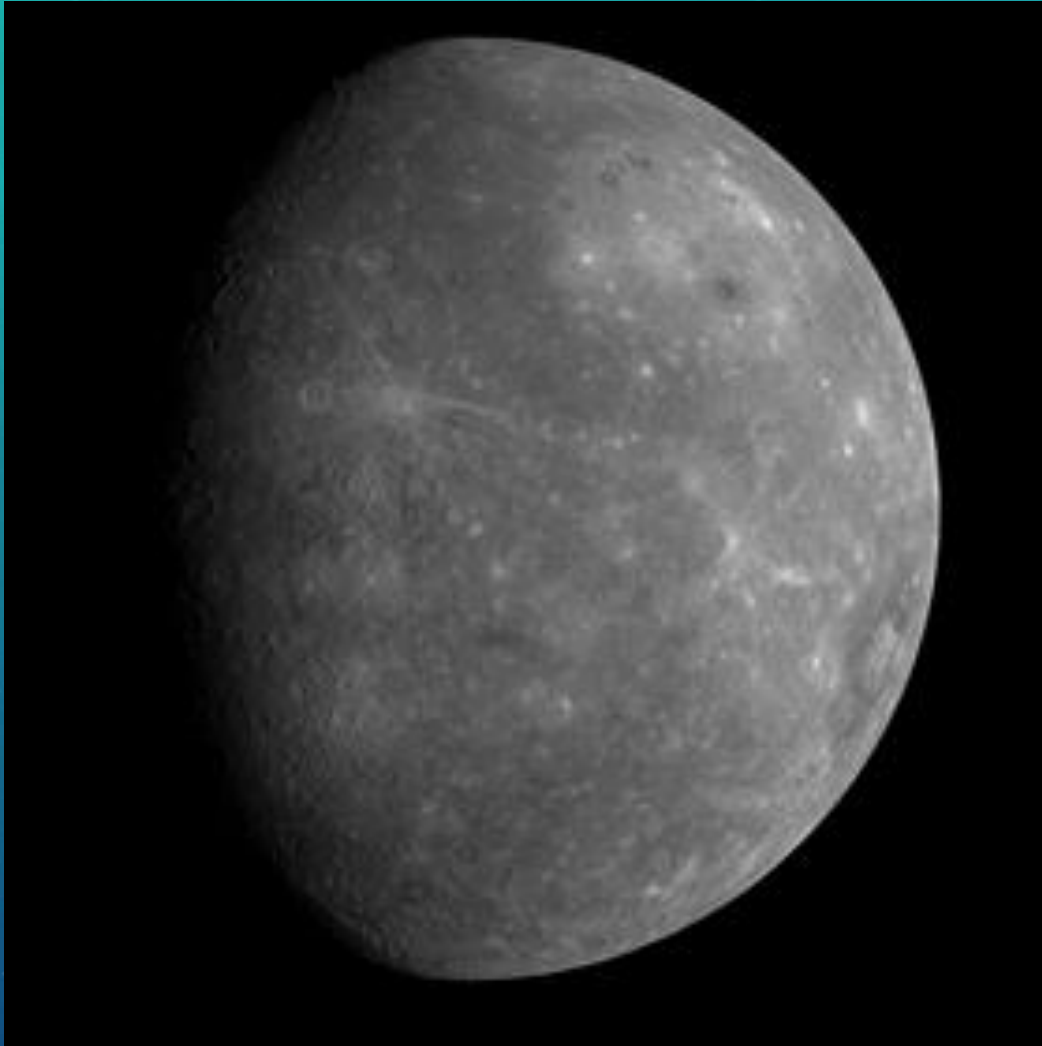
Launched on 20 October 2018



©2018 ESA-CNES-ARIANESPACE/Optique Vidéo du CSG - JIM GUILLOIN



MERCURY



Planet Mercury seen in the first of the three flybys of the MESSENGER probe

- **Innermost planet** in the Solar System
Difficult to reach
- **Harsh environment**
Difficult to stay
- Key for Solar System **formation** and **evolution** scenarios
Internal structure and composition, thermal evolution
- Unexpected **magnetosphere**
Magnetic field generation mechanism
- Important role in the development and subsequent tests of **general relativity**
Weak field but not so weak

MERCURY



The very famous 43''/century excess perihelion precession appears not to be directly explainable by classical celestial mechanics

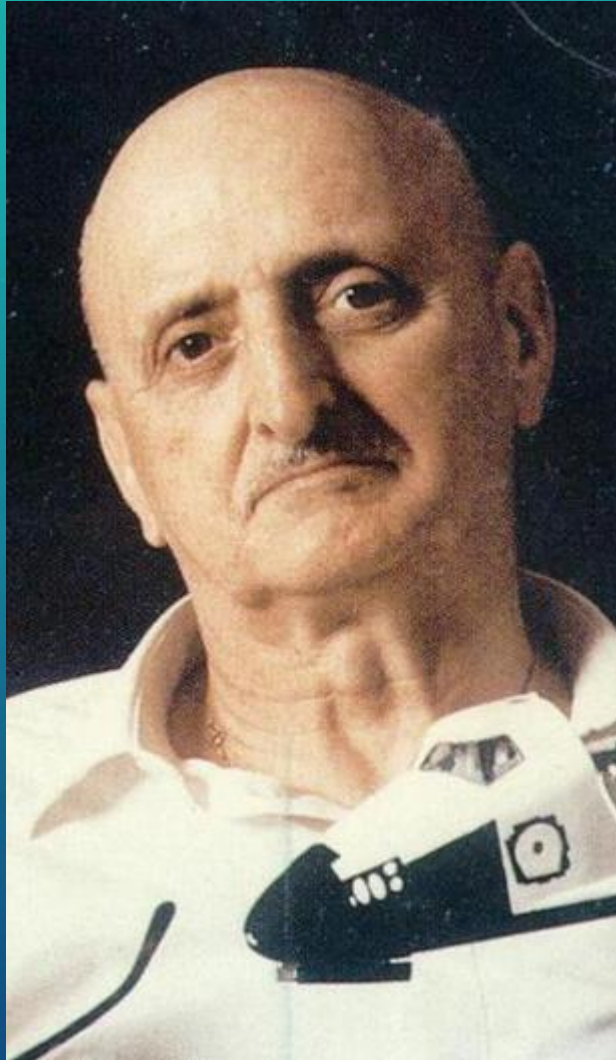
«Change the laws»

VS

«Add bodies»

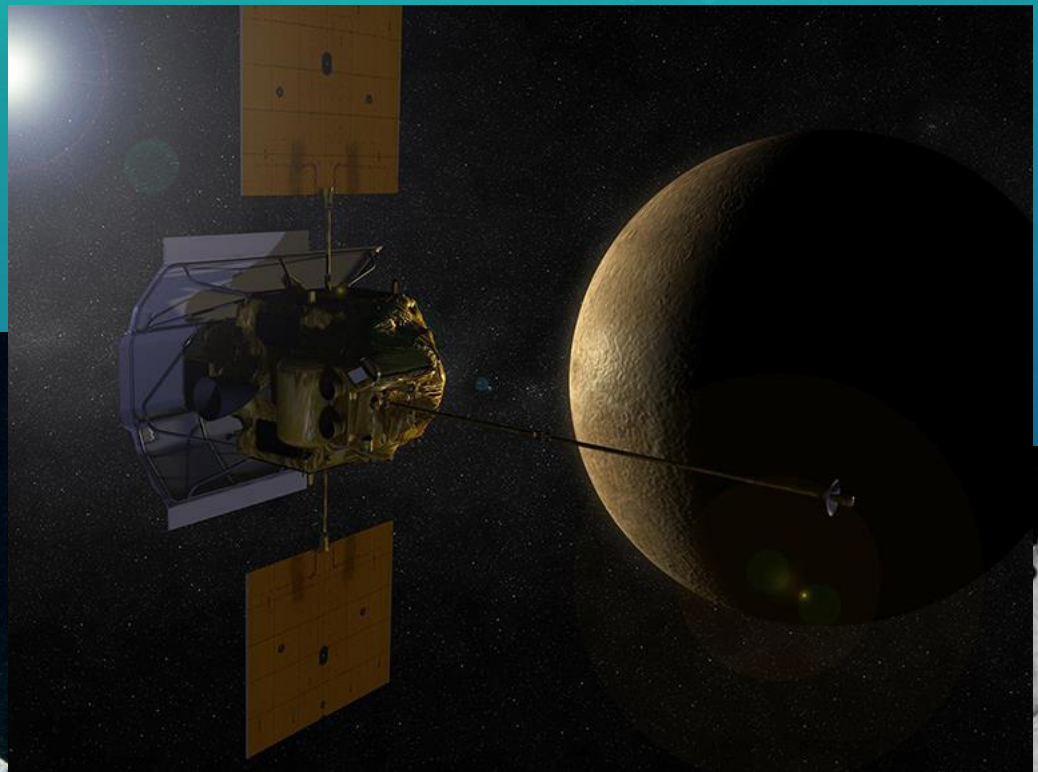
A very familiar situation (think to the so-called **dark matter**, **dark energy**...)

GIUSEPPE COLOMBO



- Found and explored with Irwin Shapiro the peculiar **3:2 resonance** between revolution and rotation periods of Mercury
- Contributed in a crucial way to **Mariner 10 trajectory design**
- Contributed to the **Giotto probe** development
- Idea of a **solar probe** («Shoot an arrow to the Sun»...)
- Contributed with Mario Grossi to the development of **tethered satellites**
- ...

MERCURY EXPLORATION



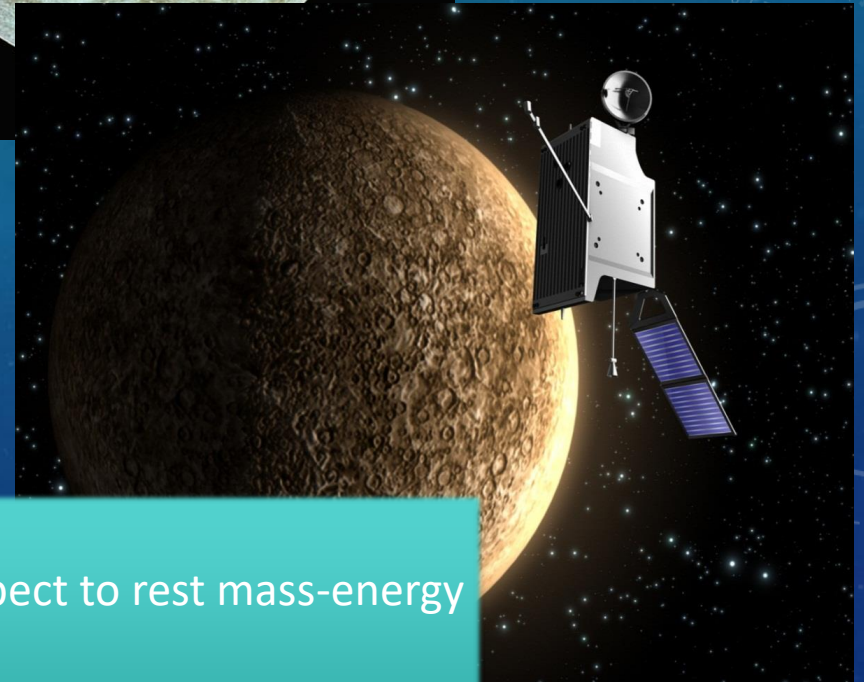
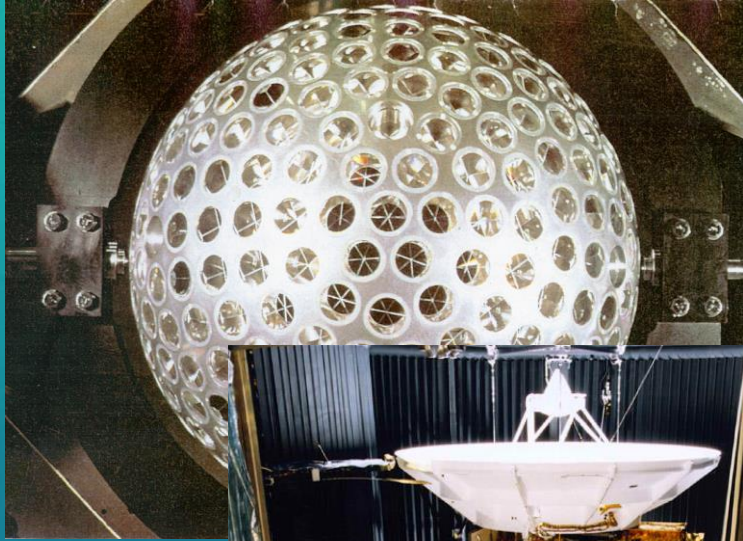
<https://solarsystem.nasa.gov/missions>
<https://sci.esa.int>

BARICENTRIC PPN EQUATIONS OF MOTION

$$\begin{aligned}\ddot{\mathbf{r}}_i = & \sum_{j \neq i} \frac{\mu_j (\mathbf{r}_j - \mathbf{r}_i)}{r_{ij}^3} \left\{ 1 - \frac{2(\beta + \gamma)}{c^2} \sum_{l \neq i} \frac{\mu_l}{r_{il}} - \frac{2\beta - 1}{c^2} \sum_{k \neq j} \frac{\mu_k}{r_{jk}} \right. \\ & + \gamma \left(\frac{\dot{s}_i}{c} \right)^2 + (1 + \gamma) \left(\frac{\dot{s}_j}{c} \right)^2 - \frac{2(1 + \gamma)}{c^2} \dot{\mathbf{r}}_i \cdot \dot{\mathbf{r}}_j \\ & \left. - \frac{3}{2c^2} \left[\frac{(\mathbf{r}_i - \mathbf{r}_j) \cdot \dot{\mathbf{r}}_j}{r_{ij}} \right]^2 + \frac{1}{2c^2} (\mathbf{r}_j - \mathbf{r}_i) \cdot \ddot{\mathbf{r}}_j \right\} \\ & + \frac{1}{c^2} \sum_{j \neq i} \frac{\mu_j}{r_{ij}^3} \left\{ [\mathbf{r}_i - \mathbf{r}_j] \cdot [(2 + 2\gamma) \dot{\mathbf{r}}_i - (1 + 2\gamma) \dot{\mathbf{r}}_j] \right\} (\dot{\mathbf{r}}_i - \dot{\mathbf{r}}_j) \\ & + \frac{3 + 4\gamma}{2c^2} \sum_{j \neq i} \frac{\mu_j \ddot{\mathbf{r}}_j}{r_{ij}}\end{aligned}$$

Moyer 2000

TEST MASS



- No electric charge
- Gravitational binding energy negligible with respect to rest mass-energy
- Angular momentum negligible
- Sufficiently small to neglect tidal effects

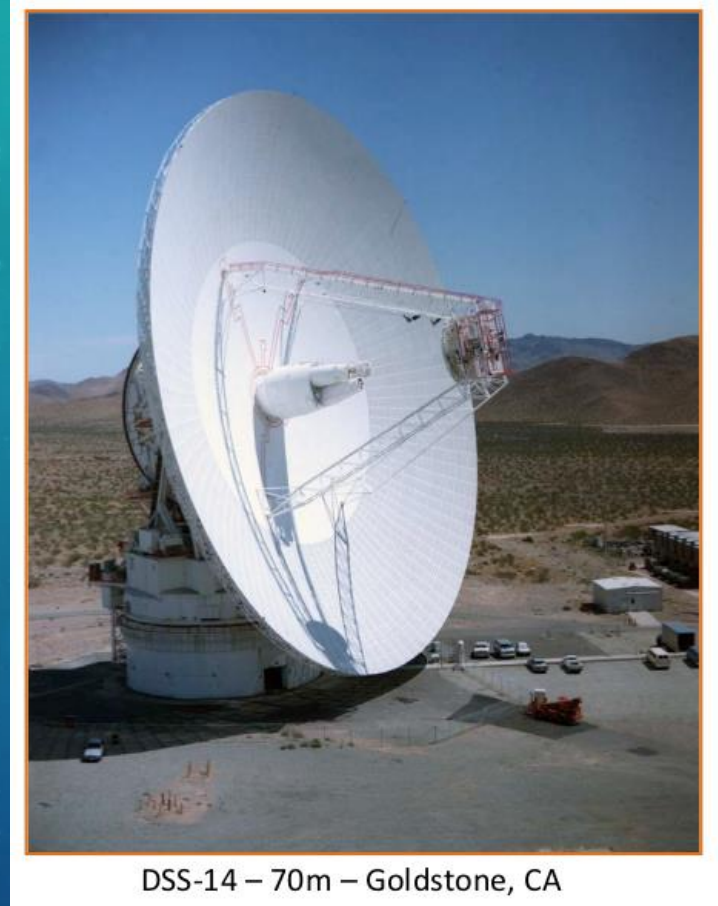
TRACKING – RADIOMETRIC

Microwave signals are exchanged between ground stations and an on-board transponder. By very precise frequency standards, range and range-rate can be derived.

$$f_R = \left(1 - \frac{\dot{\rho}}{c}\right) f_T$$

Doppler shift

In practice, the total phase change is measured. The Doppler count provides a measure of range change during integration time T_c .



JPL

- Very complex system (both ground and space segment)
- 24 hr coverage (DSN)
- Observables: range, sub-m precision; range-rate, $\sim 10^{-5} \text{ ms}^{-1}$ precision
- POD: sub-m (depends on model choices)

TRACKING – RADIOMETRIC

Microwave signals are exchanged between ground stations and an on-board transponder. By very precise frequency standards, range and range-rate can be derived.

$$f_R = \left(1 - \frac{\dot{\rho}}{c}\right) f_T$$

Doppler shift

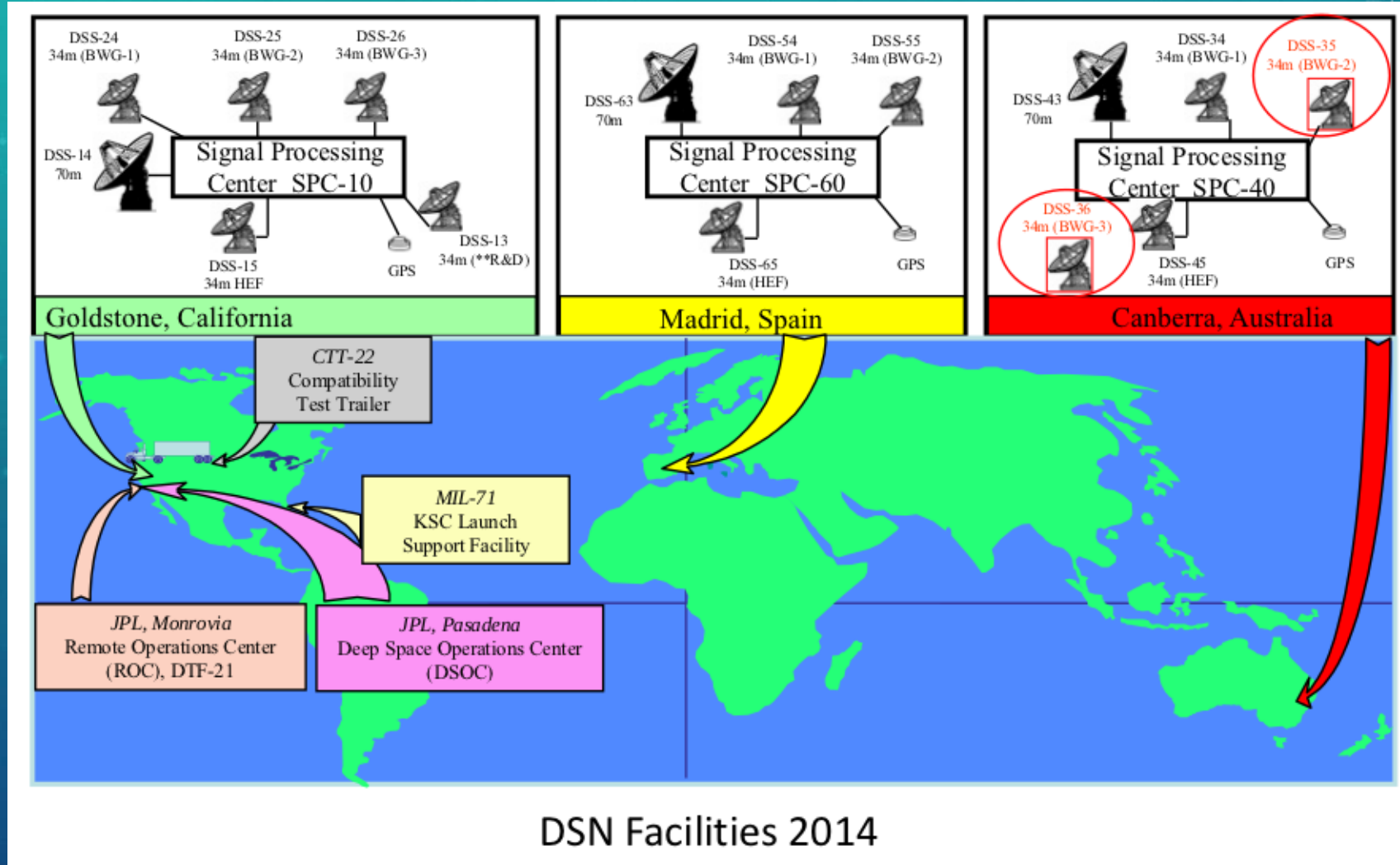
In practice, the total phase change is measured. The Doppler count provides a measure of range change during integration time T_c .

- Very complex system (both ground and space segment)
- 24 hr coverage (DSN)
- Observables: range, sub-m precision; range-rate, $\sim 10^{-5} \text{ ms}^{-1}$ precision
- POD: sub-m (depends on model choices)

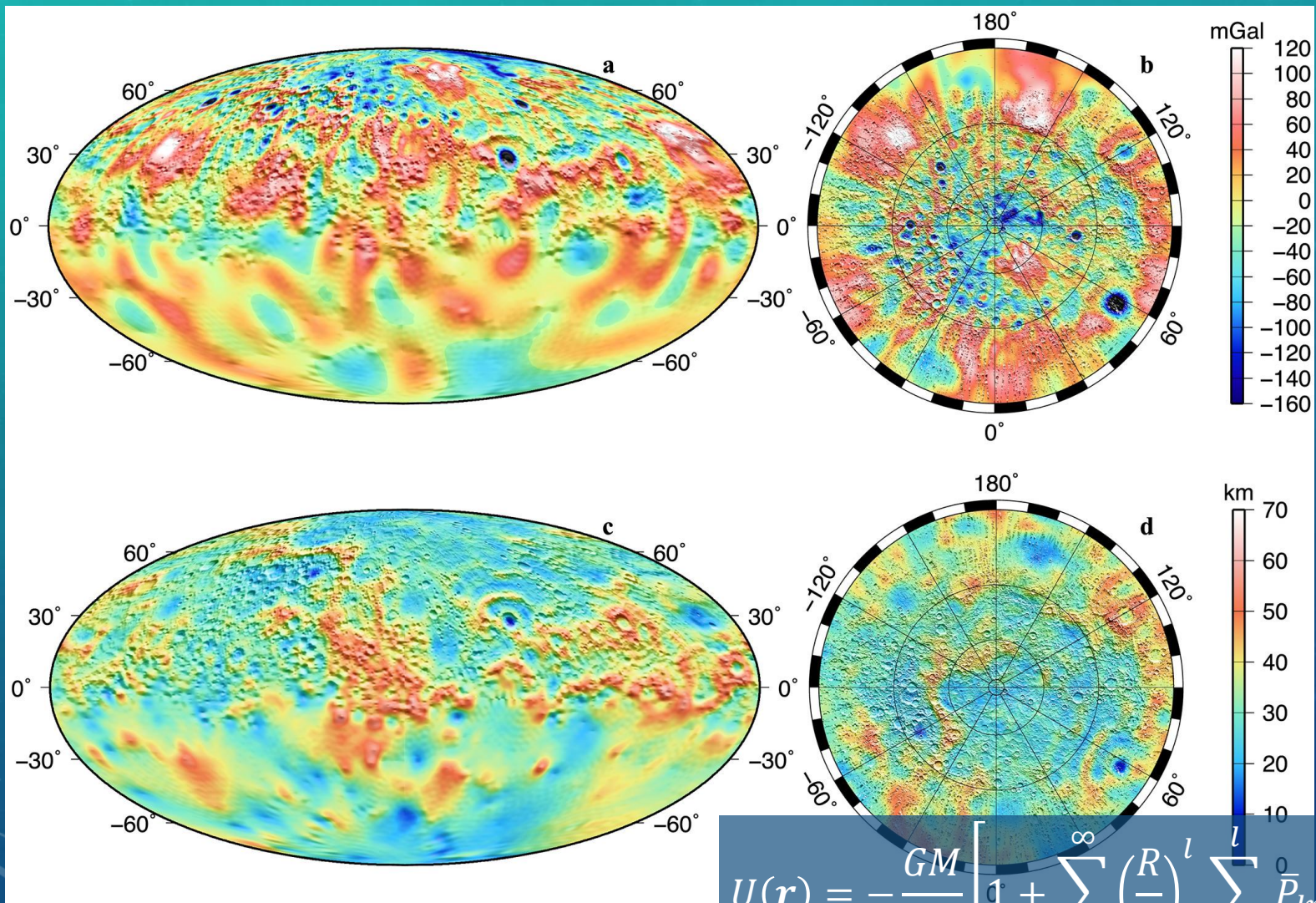
Table 3-3. Radiometric measurement system error characteristics.

Error Source	Magnitude		
	1980 S-Band	1992 X-Band	2000 X-Band
Random error for 60-s average			
Doppler	1 mm/s	0.03 mm/s	0.03 mm/s
Range	200 cm	60 cm	60 cm
Instrument bias (range)	5 m	5 m	2 m
Instrument stability @ 8 h	10^{-13}	10^{-14}	10^{-14}
Station locations			
Spin radius	100 cm	10 cm	3 cm
Longitude	100 cm	10 cm	3 cm
Baseline components	30 cm	5 cm	2 cm
Earth orientation			
(1-d prediction)	100 cm	30 cm	7 cm
Earth orientation (after the fact)	20 cm	3 cm	1 cm
Troposphere			
Zenith bias	4.5 cm	4.5 cm	1 cm
Line-of-sight fluctuation (over 10 min at 15-deg elevation)	1 cm	1 cm	1 cm
Ionosphere (line of sight, above 10 deg)			
	100 cm	3 cm	3 cm
Solar plasma			
20-deg Sun-Earth-probe angle			
Total line of sight	229 m	17 m	17 m
Drift over 8 h	15 m	115 cm	115 cm
Station-differenced	7 cm	0.5 cm	0.5 cm
180-deg Sun-Earth-probe angle			
Total line of sight	16 m	116 cm	116 cm
Drift over 8 h	2 m	15 cm	15 cm
Station-differenced	1 cm	0.1 cm	0.1 cm
Station clock			
Epoch	1 μs	1 μs	1 μs
Rate	10^{-12}	5×10^{-14}	5×10^{-14}
Stability @ 1000 s	10^{-14}	10^{-15}	10^{-15}

TRACKING – RADIOMETRIC



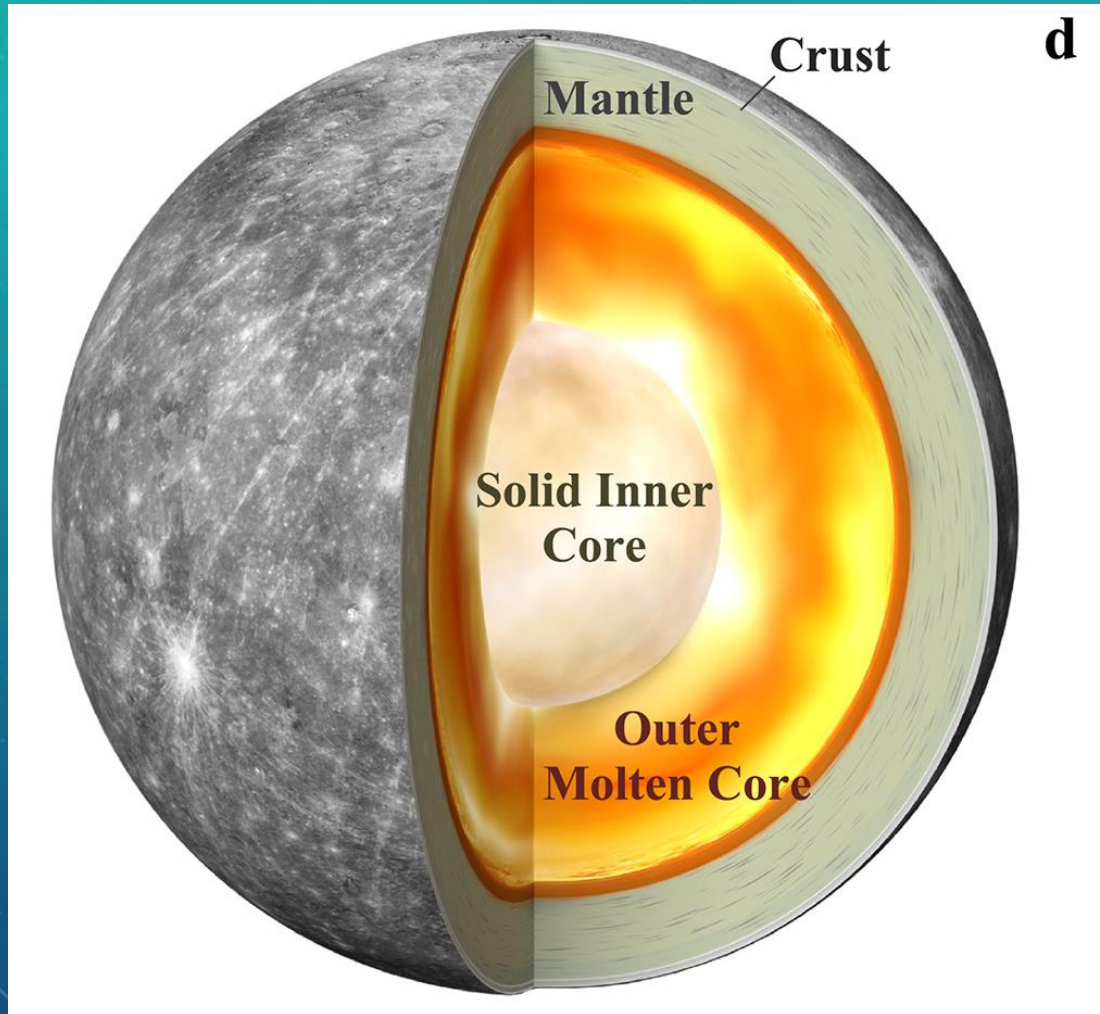
GRAVITATION AS PROBE OF PLANETARY INTERIORS



Free-air gravity anomaly and crustal thickness on Mercury from gravity field **HgM008**

$$U(r) = -\frac{GM}{r} \left[1 + \sum_{l=1}^{\infty} \left(\frac{R}{r}\right)^l \sum_{m=0}^l \bar{P}_{lm}(\cos \theta) (\bar{C}_{lm} \cos(m\phi) + \bar{S}_{lm} \sin(m\phi)) \right]$$

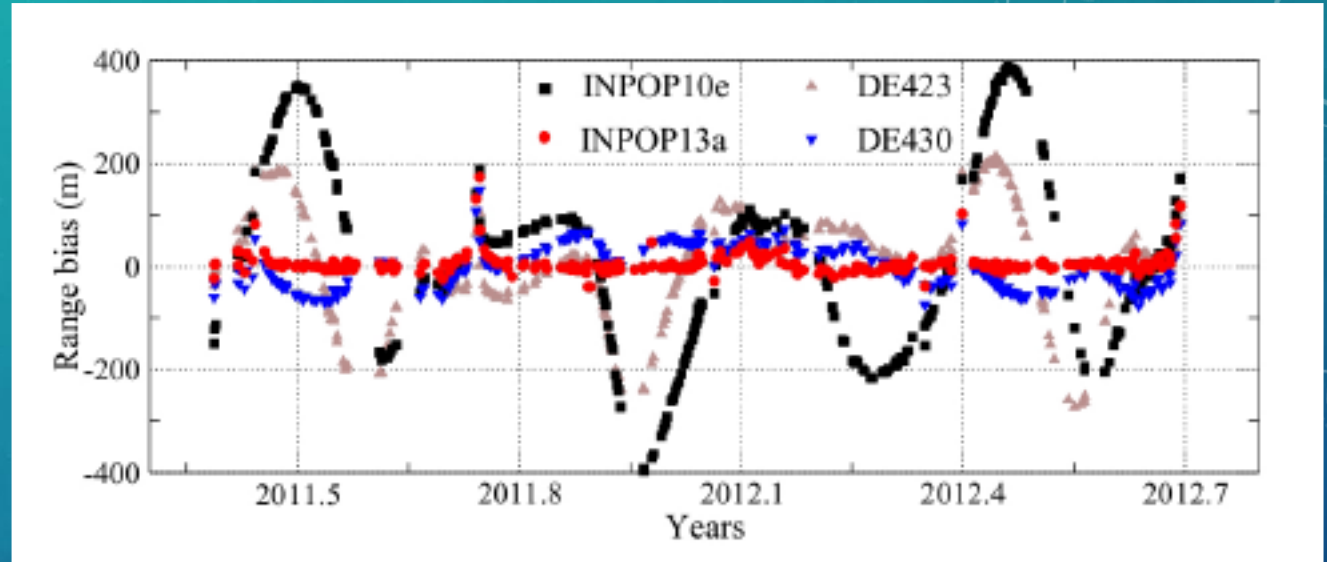
GRAVITATION AS PROBE OF PLANETARY INTERIORS



Evidence is accumulating on the existence of an outer molten core of Mercury, consistent with the presence of a weak global magnetic field

SOLAR SYSTEM EPHEMERIDES

Type of data		Nbr	Time interval	INPOP13a mean	1 σ	INPOP10e mean	1 σ
Mercury	range [m]	462	1971.29–1997.60	-108	866	-45	872
Mercury Messenger	GINS range [m]	314	2011.39–2012.69	2.8	12.0	15.4	191.8
Out from SC*	GINS range [m]	267	2011.39–2012.66	-0.4	8.4	6.2	205.2
Mercury Mariner	range [m]	2	1974.24–1976.21	-124	56	-52.5	113
Mercury flybys Mess	ra [mas]	3	2008.03–2009.74	0.85	1.35	0.73	1.48
Mercury flybys Mess	de [mas]	3	2008.03–2009.74	2.4	2.4	2.4	2.5
Mercury flybys Mess	range [m]	3	2008.03–2009.74	-1.9	7.7	-5.05	5.8
Venus	VLBI [mas]	46	1990.70–2010.86	1.6	2.6	1.6	2.6
Venus	range [m]	489	1965.96–1990.07	502	2236	500	2235
Venus Vex	range [m]	24970	2006.32–2011.45	1.3	11.9	1.1	11.9
Mars	VLBI [mas]	96	1989.13–2007.97	-0.02	0.41	-0.00	0.41
Mars Mex	range [m]	21 482	2005.17–2011.45	-2.1	20.6	-1.3	21.5
Mars MGS	GINS range [m]	13 091	1999.31–2006.83	-0.6	3.3	-0.3	3.9
Mars Ody	range [m]	5664	2006.95–2010.00	1.6	2.3	0.3	4.1
Mars Path	range [m]	90	1997.51–1997.73	6.1	14.1	-6.3	13.7
Mars Vkg	range [m]	1257	1976.55–1982.87	-0.4	36.1	-1.4	39.7
Jupiter	VLBI [mas]	24	1996.54–1997.94	-0.5	11.0	-0.3	11.0
Jupiter Optical	ra [mas]	6532	1914.54–2008.49	-40	297	-39	297
Jupiter Optical	de [mas]	6394	1914.54–2008.49	-48	301	-48	301
Jupiter flybys	ra [mas]	5	1974.92–2001.00	2.6	2.9	2.4	3.2
Jupiter flybys	de [mas]	5	1974.92–2001.00	-11.0	11.5	-10.8	11.5
Jupiter flybys	range [m]	5	1974.92–2001.00	-1065	1862	-907	1646
Saturne Optical	ra [mas]	7971	1913.87–2008.34	-6	293	-6	293
Saturne Optical	de [mas]	7945	1913.87–2008.34	-12	266	-2	266
Saturne VLBI Cass	ra [mas]	10	2004.69–2009.31	0.19	0.63	0.21	0.64
Saturne VLBI Cass	de [mas]	10	2004.69–2009.31	0.27	0.34	0.28	0.33
Saturne Cassini	ra [mas]	31	2004.50–2007.00	0.8	3.4	0.8	3.9
Saturne Cassini	de [mas]	31	2004.50–2007.00	6.5	7.2	6.5	7.2
Saturne Cassini	range [m]	31	2004.50–2007.00	-0.010	18.44	-0.013	18.84
Uranus Optical	ra [mas]	13 016	1914.52–2011.74	7	205	7	205
Uranus Optical	de [mas]	13 008	1914.52–2011.74	-6	234	-6	234
Uranus flybys	ra [mas]	1	1986.07–1986.07	-21		-21	
Uranus flybys	de [mas]	1	1986.07–1986.07	-28		-28	
Uranus flybys	range [m]	1	1986.07–1986.07	20.7		19.7	
Neptune Optical	ra [mas]	5395	1913.99–2007.88	2	258	0.0	258
Neptune Optical	de [mas]	5375	1913.99–2007.88	-1	299	-0.0	299
Neptune flybys	ra [mas]	1	1989.65–1989.65	-12		-12	
Neptune flybys	de [mas]	1	1989.65–1989.65	-5		-5	
Neptune flybys	range [m]	1	1989.65–1989.65	66.8		69.6	
Pluto Optical	ra [mas]	2438	1914.06–2008.49	-186	664	34	654
Pluto Optical	de [mas]	2461	1914.06–2008.49	11	536	7	539
Pluto Occ	ra [mas]	13	2005.44–2009.64	6	49	3	47
Pluto Occ	de [mas]	13	2005.44–2009.64	-7	18	-6	18
Pluto HST	ra [mas]	5	1998.19–1998.20	-42	43	33	43
Pluto HST	de [mas]	5	1998.19–1998.20	31	48	28	48
Venus Vex**	range [m]	2827	2011.45–2013.00	51	124	52	125
Mars Mex**	range [m]	4628	2011.45–2013.00	-3.0	11.5	4.2	27.5



Verma+ 2008

INPOP13a: a recent ephemeris fit with a number of Solar System data, including MESSENGER tracking

BEPICOLOMBO – MORE SCIENCE GOALS



The **Mercury Orbiter Radio Science Experiment (MORE)** uses the BepiColombo radiometric tracking measurements from ground antennas to precisely locate (position and velocity) the spacecraft and obtain informations on the gravitational dynamics environment

Involved instruments:

- **Ka-band transponder**
- Star Tracker
- High-resolution camera
- **Accelerometer**

- **Gravity** High-fidelity determination of static gravity field and gravitational tidal response (Love number k_2) of Mercury
- **Rotation** Estimation of Mercury's rotational state (pole orientation, spin rate, amplitude and phase of physical librations in longitude)
- **Fundamental physics** Test different aspects of general relativity through a precise determination of several parameterized post-Newtonian parameters

BEPICOLOMBO – MORE SCIENCE GOALS

Gravity and rotation

- **Static gravity field** to maximum degree and order 45 (or 35 when Kaula regularization is not used) to constrain the **properties of the crust and the lithosphere**, accounting for Mercury's internal loading
- **Subsurface properties** of Mercury to infer the **internal heat flow** at different epochs
- **Tidal variations of the gravity field** through the estimation of the Love number k_2 , which, in combination with the Love number h_2 and the measurements of the **rotational state**, allows determining the **state and dimension of the liquid outer core and the solid inner core**
- **Principal moments of inertia** of Mercury by estimating the low degree gravity coefficients C_{20} and C_{22} , the librations and pole obliquity to better characterize the **deep interior**



BEPICOLOMBO – MORE SCIENCE GOALS

Gravity and rotation

$$\frac{C_{\text{cr/m}}}{C} = \frac{C_{\text{cr/m}}}{B - A} \frac{B - A}{MR^2} \frac{MR^2}{C}$$

Peale's formula (is core decoupled from crust/mantle?)



BEPICOLOMBO – MORE SCIENCE GOALS

Gravity and rotation

$$\frac{C_{\text{cr/m}}}{C} = \frac{C_{\text{cr/m}}}{B - A} \frac{B - A}{MR^2} \frac{MR^2}{C}$$

Peale's formula (is core decoupled from crust/mantle?)

Amplitude of the forced librations in longitude

BEPICOLOMBO – MORE SCIENCE GOALS

Gravity and rotation

$$\frac{C_{cr/m}}{C} = \frac{C_{cr/m}}{B-A} \frac{B - AMR^2}{MR^2} \frac{1}{C}$$

Peale's formula (is core decoupled from crust/mantle?)

C_{22} Stokes coefficient

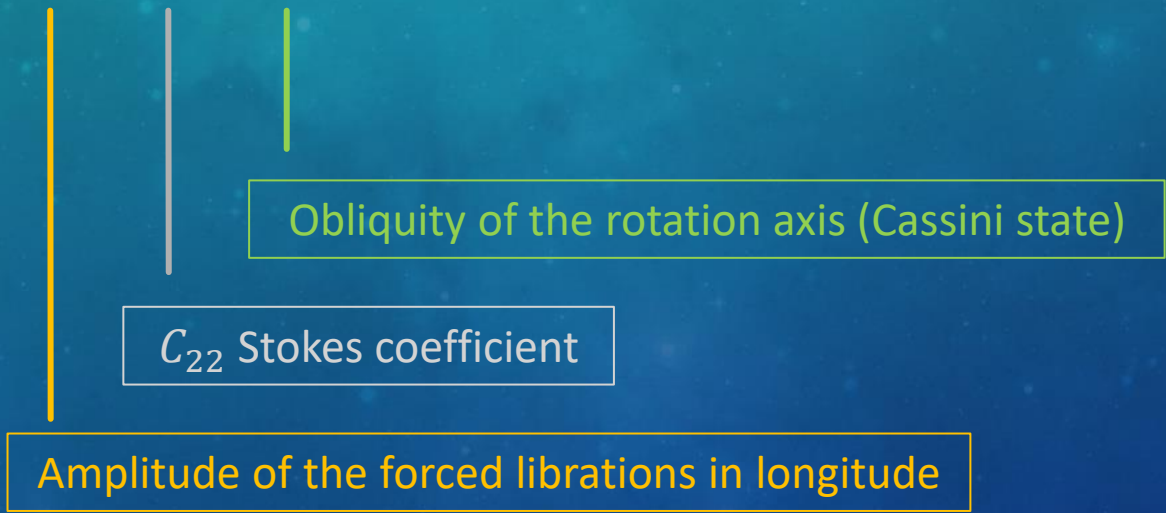
Amplitude of the forced librations in longitude

BEPICOLOMBO – MORE SCIENCE GOALS

Gravity and rotation

$$\frac{C_{cr/m}}{C} = \frac{C_{cr/m}}{B-A} \frac{B - A}{MR^2} \frac{MR^2}{C}$$

Peale's formula (is core decoupled from crust/mantle?)



BEPICOLOMBO – MORE SCIENCE GOALS

Fundamental Physics

- Test **general relativity and alternative theories of gravitation** to a level better than 10^{-5} by measuring the **time delay and Doppler shift of radio waves**, and the **precession of Mercury's perihelion**
- Test the **strong equivalence principle** to a level better than 4×10^{-5}
- Test the **isotropy of space and preferred frame effects**
- Determine dynamically the **gravitational oblateness of the Sun** (C_{20}) to better than 10^{-8}
- Set improved upper limits to the **time variation of the gravitational “constant” G**
- Set upper limits to the **Compton wavelength of the graviton**



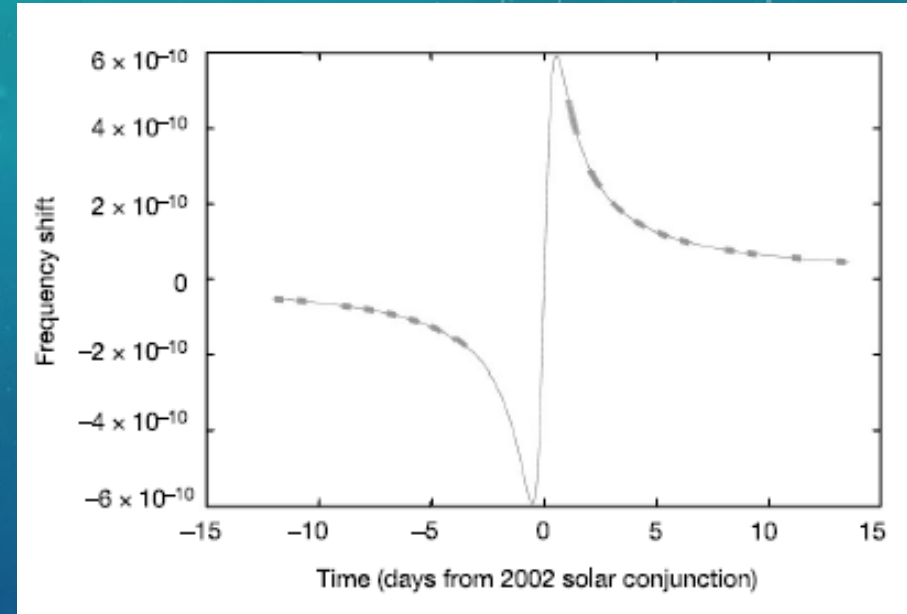
CLASSICAL TESTS

Round trip time:

$$\Delta t = 2(1 + \gamma) \frac{GM_{\odot}}{c^3} \ln \left(\frac{4r_1 r_2}{b^2} \right)$$

Frequency shift of photons:

$$\frac{\Delta \nu}{\nu} = \frac{d\Delta t}{dt} = -2(1 + \gamma) \frac{GM_{\odot}}{c^3 b} \frac{db}{dt}$$

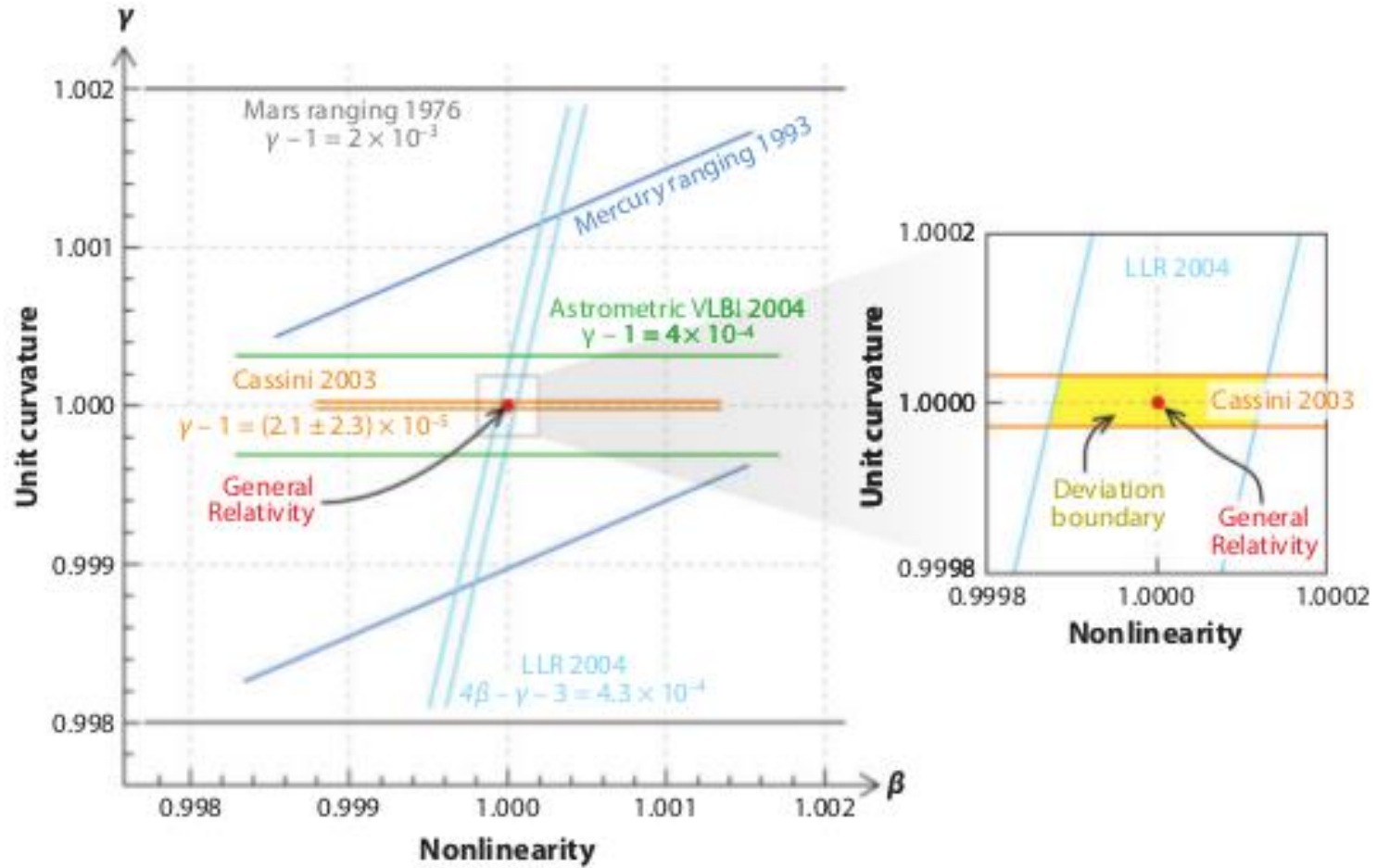


Bertotti+ 2003

Best result from Cassini:

$$\gamma = 1 + (2.1 \pm 2.3) \times 10^{-5}$$

CLASSICAL TESTS



BEPICOLOMBO – EXPECTED IMPROVEMENTS

Table 4: Current limits on the PPN parameters.

Parameter	Effect	Limit	Remarks
$\gamma - 1$	time delay	2.3×10^{-5}	Cassini tracking
	light deflection	2×10^{-4}	VLBI
$\beta - 1$	perihelion shift	8×10^{-5}	$J_{2\odot} = (2.2 \pm 0.1) \times 10^{-7}$
	Nordtvedt effect	2.3×10^{-4}	$\eta_N = 4\beta - \gamma - 3$ assumed
ξ	spin precession	4×10^{-9}	millisecond pulsars
α_1	orbital polarization	10^{-4}	Lunar laser ranging
		4×10^{-5}	PSR J1738+0333
α_2	spin precession	2×10^{-9}	millisecond pulsars
α_3	pulsar acceleration	4×10^{-20}	pulsar \dot{P} statistics
ζ_1	—	2×10^{-2}	combined PPN bounds
ζ_2	binary acceleration	4×10^{-5}	\ddot{P}_p for PSR 1913+16
ζ_3	Newton's 3rd law	10^{-8}	lunar acceleration
ζ_4	—	—	not independent [see Eq. (73)]

Table 5 Comparison of expected accuracies in PPN parameters, gravitational parameter of the sun, relative time derivative of the Newtonian gravitational constant, and Compton wavelength of the graviton, using different assumptions in the analysis (see text). (From De Marchi and Cascioli 2020)

Parameter	Nominal mission	Extended mission	
	Imperi et al.	Imperi et al.	De Marchi and Cascioli
γ	1.1×10^{-6}	6.6×10^{-7}	1.0×10^{-6}
β	1.0×10^{-6}	4.5×10^{-7}	1.7×10^{-5}
J_2	5.5×10^{-10}	1.37×10^{-9}	2.8×10^{-9}
η	3.0×10^{-6}	1.36×10^{-6}	6.9×10^{-5}
α_1	6.1×10^{-7}	1.2×10^{-7}	3.4×10^{-7}
α_2	1.3×10^{-7}	4.6×10^{-8}	6.7×10^{-8}
GM_{\odot} ($\text{km}^3 \text{s}^{-2}$)	.053	0.015	0.08
ζ (yr^{-1})	2.8×10^{-14}	3.2×10^{-15}	9.2×10^{-15}
λ_g (km)	—	—	1.1×10^{14}

Will 2014

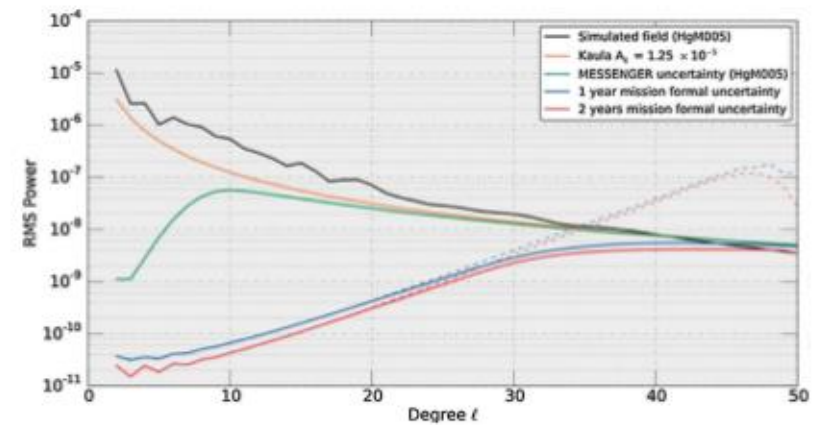


Fig. 9 MORE estimate of gravity field in terms of power associated with degree l . The formal error spectrum is reported for both the nominal and the extended mission. Dotted lines give the error spectrum when the Kaula regularization is not used. (From Imperi et al. 2018)

BEPICOLOMBO – EXPECTED IMPROVEMENTS

Table 4: Current limits on the PPN parameters.

Parameter	Effect	Limit	Remarks
$\gamma - 1$	time delay	2.3×10^{-5}	Cassini tracking
	light deflection	2×10^{-4}	VLBI
$\beta - 1$	perihelion shift	8×10^{-5}	$J_{2\odot} = (2.2 \pm 0.1) \times 10^{-7}$
	Nordtvedt effect	2.3×10^{-4}	$\eta_N = 4\beta - \gamma - 3$ assumed
ξ	spin precession	4×10^{-9}	millisecond pulsars
α_1	orbital polarization	10^{-4}	Lunar laser ranging
		4×10^{-5}	PSR J1738+0333
α_2	spin precession	2×10^{-9}	millisecond pulsars
α_3	pulsar acceleration	4×10^{-20}	pulsar \dot{P} statistics
ζ_1	—	2×10^{-2}	combined PPN bounds
ζ_2	binary acceleration	4×10^{-5}	\ddot{P}_p for PSR 1913+16
ζ_3	Newton's 3rd law	10^{-8}	lunar acceleration
ζ_4	—	—	not independent [see Eq. (73)]

Table 5 Comparison of expected accuracies in PPN parameters, gravitational parameter of the sun, relative time derivative of the Newtonian gravitational constant, and Compton wavelength of the graviton, using different assumptions in the analysis (see text). (From De Marchi and Cascioli 2020)

Parameter	Nominal mission	Extended mission	
	Imperi et al.	Imperi et al.	De Marchi and Cascioli
γ	1.1×10^{-6}	6.6×10^{-7}	1.0×10^{-6}
β	1.0×10^{-6}	4.5×10^{-7}	1.7×10^{-5}
J_2	5.5×10^{-10}	1.37×10^{-9}	2.8×10^{-9}
η	3.0×10^{-6}	1.36×10^{-6}	6.9×10^{-5}
α_1	6.1×10^{-7}	1.2×10^{-7}	3.4×10^{-7}
α_2	1.3×10^{-7}	4.6×10^{-8}	6.7×10^{-8}
GM_{\odot} ($\text{km}^3 \text{s}^{-2}$)	.053	0.015	0.08
ζ (yr^{-1})	2.8×10^{-14}	3.2×10^{-15}	9.2×10^{-15}
λ_g (km)	—	—	1.1×10^{14}

Will 2014

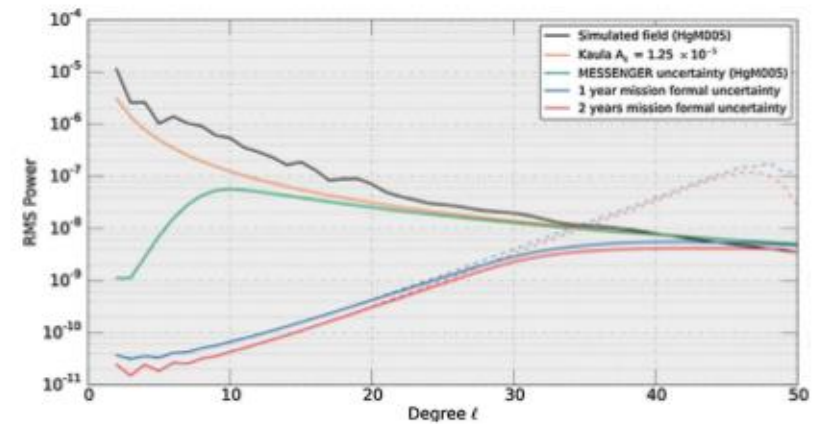


Fig. 9 MORE estimate of gravity field in terms of power associated with degree l . The formal error spectrum is reported for both the nominal and the extended mission. Dotted lines give the error spectrum when the Kaula regularization is not used. (From Imperi et al. 2018)

ON THE WAY TO MERCURY

Class. Quantum Grav. 34 (2017) 075002

L Imperi and L less

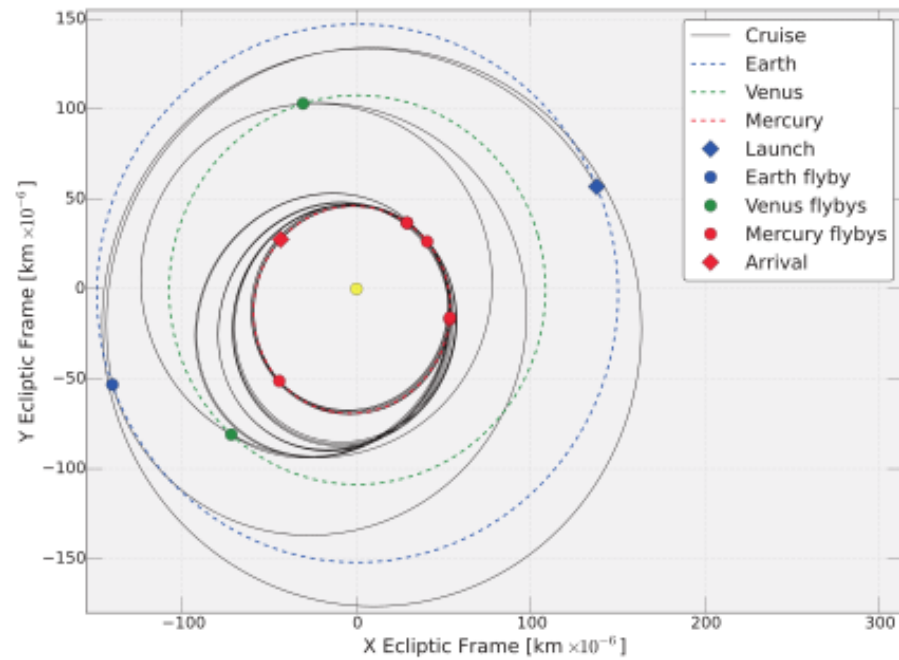
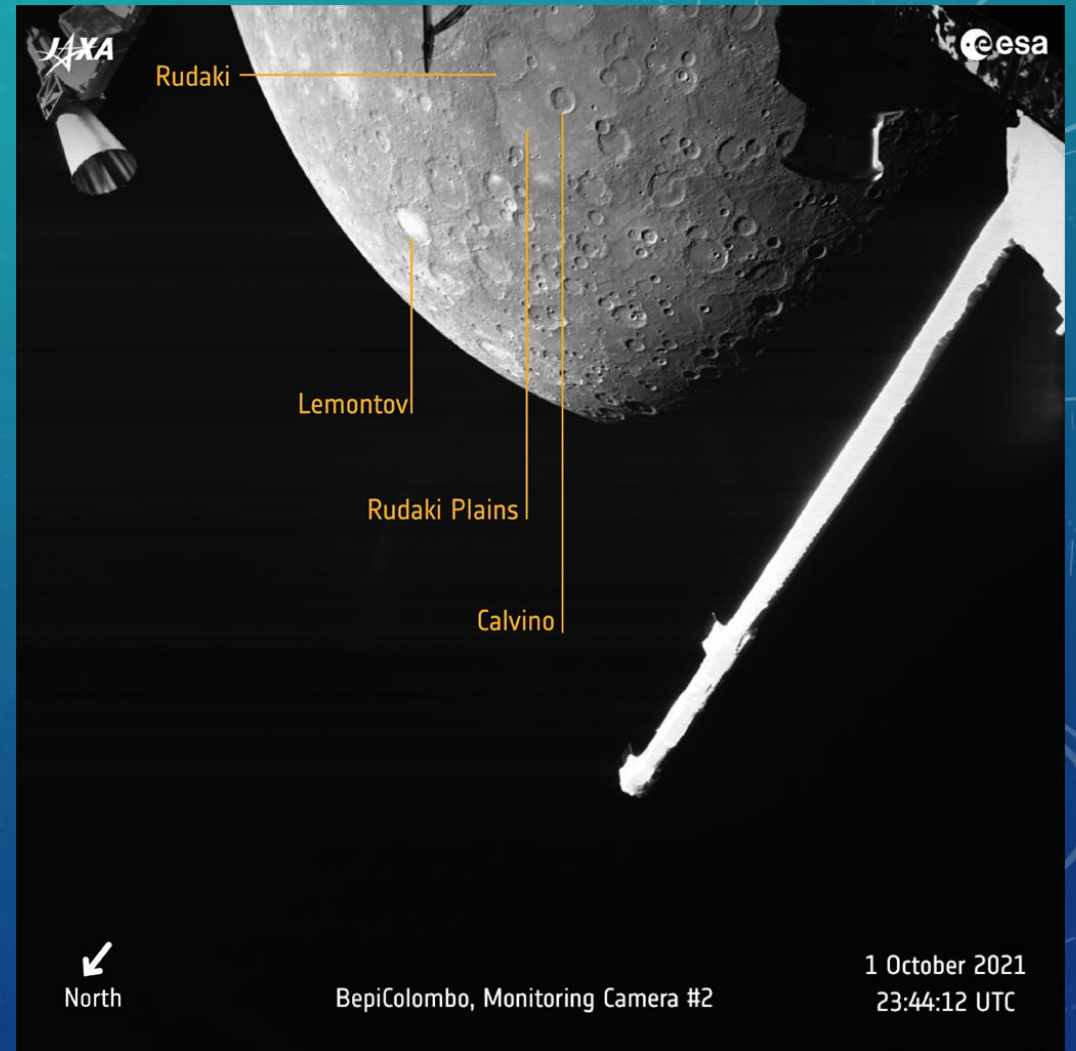


Figure 2. The cruise phase of BepiColombo, projected on the Ecliptic plane.

Imperi+less 2017

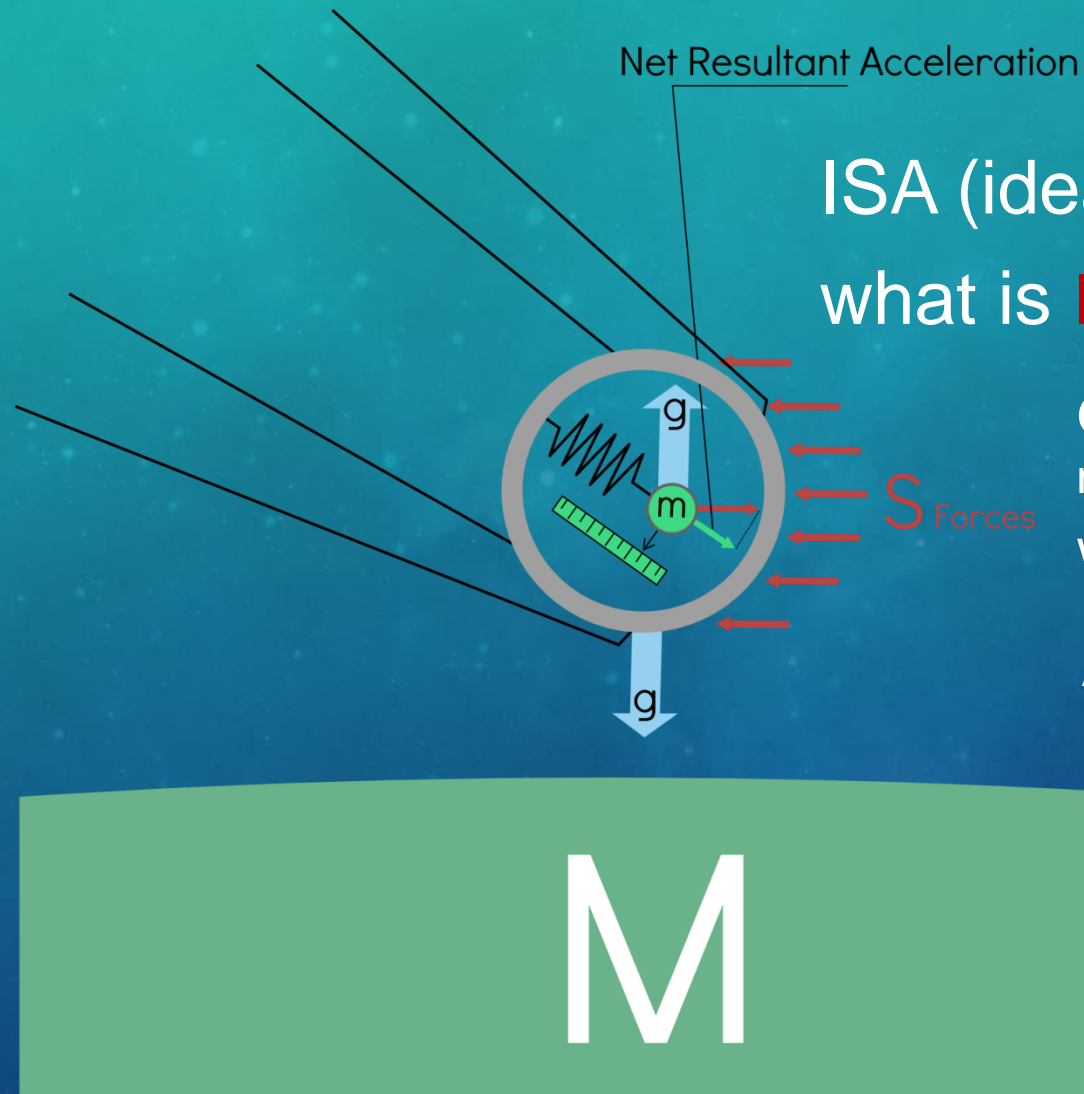


North

BepiColombo, Monitoring Camera #2

1 October 2021
23:44:12 UTC

ACCELERATION MEASUREMENTS

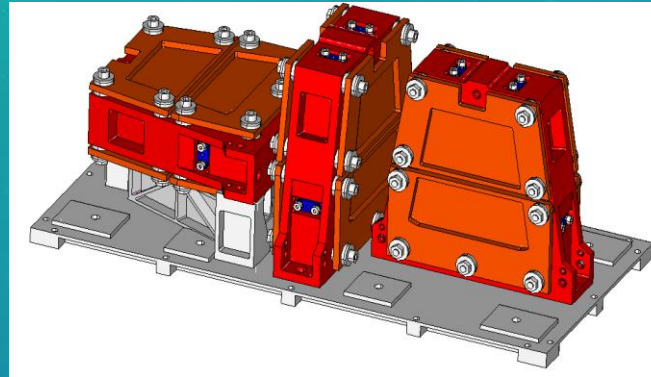


ISA (ideally!) measures only what is **not** caused by **gravity**

Gravity (ideally!) acts on the sensing mass and the satellite structure with the same acceleration

All other **NGA (S)** don't

ITALIAN SPRING ACCELEROMETER



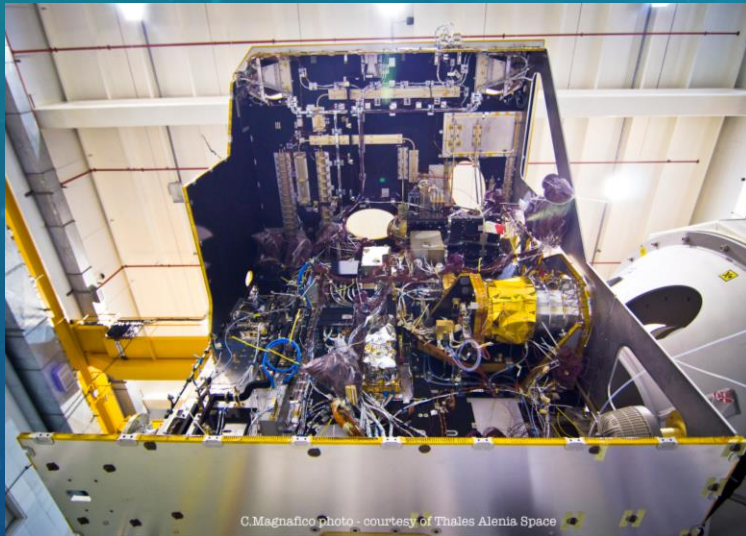
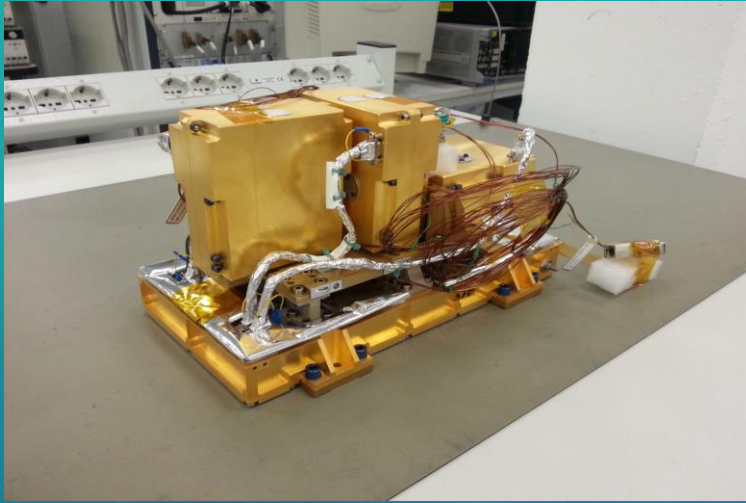
ISA oscillator parameters:	
Mass	200 g
Resonance frequency	3.9 Hz
Mechanical quality factor	10

ISA thermal stability:		
Sensor thermal sensitivity	5×10^{-7}	m/s ² /°C
Electronic thermal sensitivity	1×10^{-8}	m/s ² /°C
Active thermal control attenuation	700	

ISA performance:	
Measurement bandwidth	$3 \times 10^{-5} - 1 \times 10^{-1}$ Hz
Intrinsic noise	1×10^{-9} m/s ² /√Hz
Measurement accuracy	1×10^{-8} m/s ²
Dynamics	300×10^{-8} m/s ²
A/D converter saturation	3000×10^{-8} m/s ²

Temperature variations:	
Mercury half sidereal period (44 days)	25°C peak-to-peak
MPO orbital period (2.325 h)	4°C peak-to-peak
Random noise	10°C /√Hz

ITALIAN SPRING ACCELEROMETER



C.Magnafico photo - courtesy of Thales Alenia Space



C.Magnafico photo - courtesy of Thales Alenia Space



ITALIAN SPRING ACCELEROMETER



ISA «first light»

DTU-E101-08 D1

USER: USER_026 | vmbcd22 | PRIME@bmc1 | PARC_FLIGHT_BC

TC History - vmbcd22 - BC

Start	Description	Sequence	Dir	Release Time	Execution Time	Seq	Fs	3	U	C	5	4	31	Source	PC	TC	OK	OK	CC	Last	St	Co	
ZBL03129	BELA HK Parameter Report Gen Interval	ABLF010A	BC	2018-330T13:10:07.001	2018-330T13:10:50.799	100	65	E	E	E	E			MS vmbcd07	84	01	5	555	55	55	2018-330T13:10:50.799		
ZBL18503	BELA Check Memory Segments	ABLE004A	BC	2018-330T13:10:17.053	2018-330T13:11:00.919	100	65	E	E	E	E			MS vmbcd07	85	01	5	555	55	55	2018-330T13:11:00.919		
ZCL00306	CPL Disable HK Telemetry Generation	AJXF002A	BC	2018-330T13:10:27.015	2018-330T13:11:10.806	1	13	E	E	E	E			MS vmbcd02	86	01	5	555	55	55	2018-330T13:11:10.806		
ZBLV0607	BELA Load Data to Memory (ORSM)	BC	BC	2018-330T13:26:03.833	2018-330T13:26:03.833	100	65	E	E	E	E			MS vmbcd07	87	01	5	555	55	55	2018-330T13:26:03.833		
ZSAK4160	Start OBCP: ISA ON	ASAF001A	E BC	2018-330T13:26:04.979	2018-330T13:26:48.824	125	10	E	E	E	E			MS vmbcd02	88	01	5	555	55	55	2018-330T13:26:48.824		
ZBL18532	BELA Bill Memory Using Absolute Address	BC	BC	2018-330T13:27:26.987	2018-330T13:28:10.319	100	65	E	E	E	E			MS vmbcd07	89	01	5	555	55	55	2018-330T13:28:10.319		

Domain: All | Type: | Sub-Type: | APID: | PID: | Unique ID: | Mnemonic: | Sequence: | Ack: | Workstation: Local WS | Manual Stacks | Automation System

2018-330T13:26:46 [WARNING] Audio output is not supported on this machine. The System Bell will be used as fall... note Alarm System) to propagate audible alarms to the client terminal. Contact EUD support for details on ERAS.

Command Supervisor - vmbcd22 - BC

Row	Domain	Model Host	Username	Role	Source Type	Stack Type	Num. Cmds	Status
1	BC	vmbcd08	SPACON	SPAC_001	Uplink Stack	R	0	RUNNING
10	BC	vmbcd02	SPACON	SPAC_005	Manual Stack	R	13	DISPATCHED
2	BC	vmbcd07	SPACON-B	SPAC_004	Manual Stack	R	16	RUNNING
3	BC	vmbcd08	SPACON	SPAC_001	Manual Stack	R	0	RUNNING

Command Source(10)

TC	Static PTV	Dynamic PTV	Verification	Interlock	Time Correlation
TC MaMG1	Global	ENABLED	ENABLED	NONE	ENABLED
TC TM Flow	Local	ENABLED	ENABLED	NONE	ENABLED

Status & Control

Num	Name	Description	Stat. PTV	Dyn. PTV	Release Time	U	C	E	CC	Execution Time	SeqID	Parent
1	ZSA23405	ISA (234/5) Acquire HK auxiliary data	GO	E GO	2018-330T13:29:04.993					IMMEDIATE		

26 nov 2018

RP, picture taken @ESOC, Darmstadt

ITALIAN SPRING ACCELEROMETER

Sample data taken during instrument commissioning

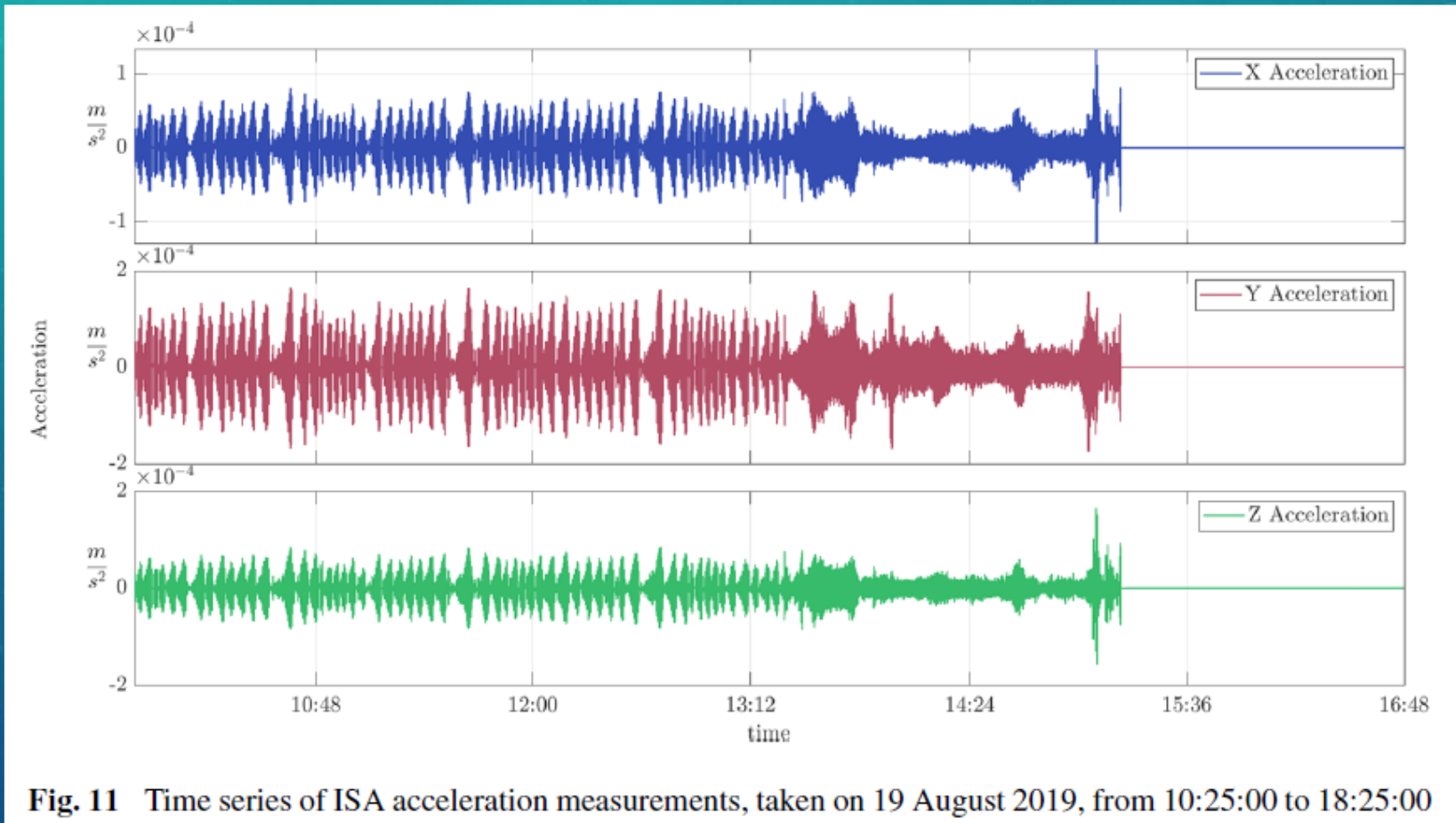


Fig. 11 Time series of ISA acceleration measurements, taken on 19 August 2019, from 10:25:00 to 18:25:00

BepiColombo ISA Science Team, Santoli+ 2020



ITALIAN SPRING ACCELEROMETER

Sample data taken during instrument commissioning

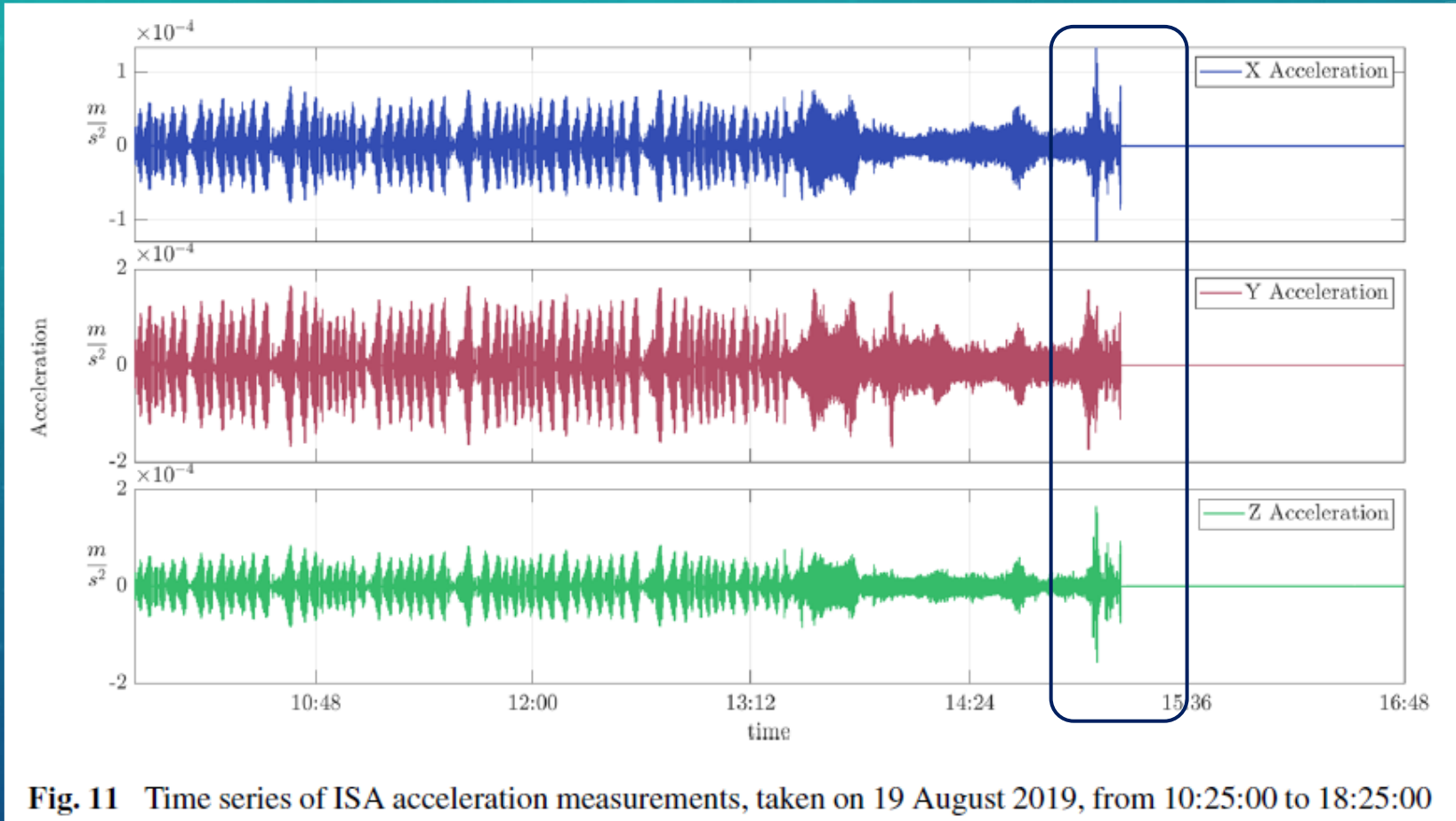


Fig. 11 Time series of ISA acceleration measurements, taken on 19 August 2019, from 10:25:00 to 18:25:00

BepiColombo ISA Science Team, Santoli+ 2020



ITALIAN SPRING ACCELEROMETER

Sample data taken during instrument commissioning

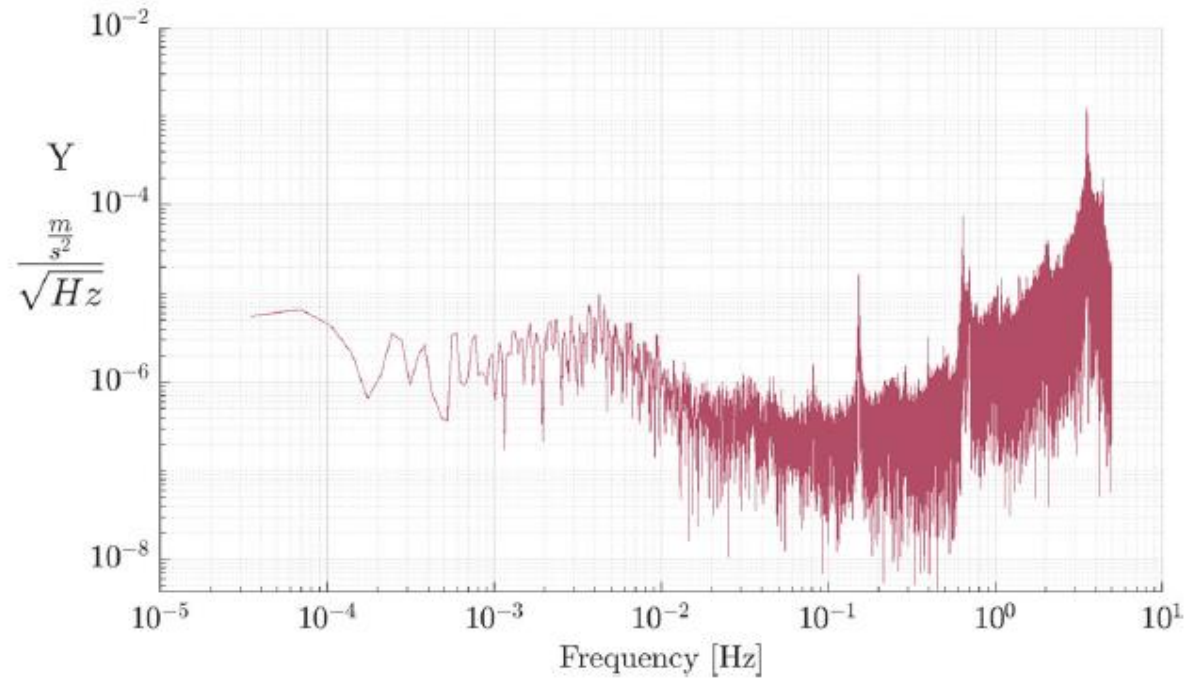


Fig. 13 ISA Normalised PSD for accelerometer 1 (ISA Y) on 19 August 2019, from 10:25:00 to 18:25:00

BepiColombo ISA Science Team, Santoli+ 2020



ITALIAN SPRING ACCELEROMETER

Sample data taken during instrument commissioning

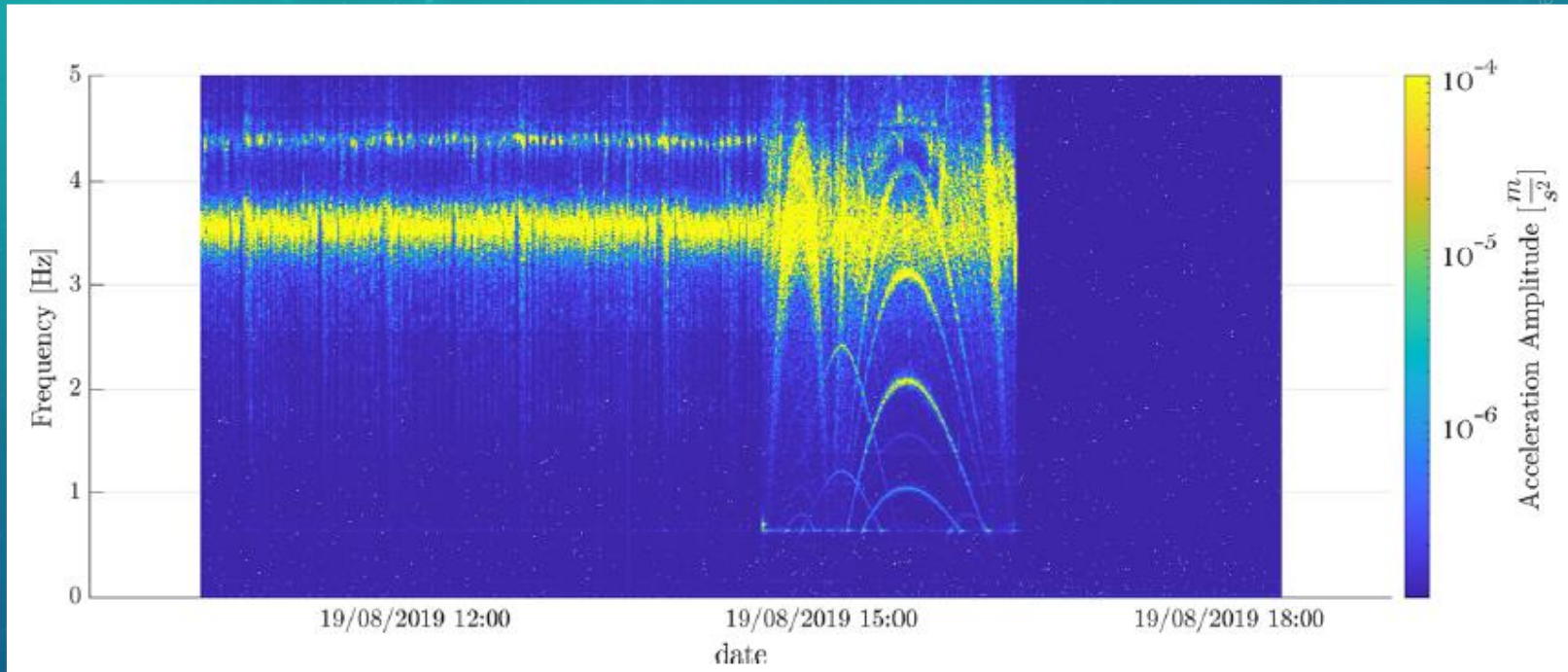


Fig. 14 ISA spectrogram for accelerometer 1 (ISA Y) on 19 August 2019, from 10:25:00 to 18:25:00. Note the signatures of the four reaction wheels from 14:35:00 to 16:27:00

BepiColombo ISA Science Team, Santoli+ 2020



ITALIAN SPRING ACCELEROMETER

Sample data taken during instrument commissioning

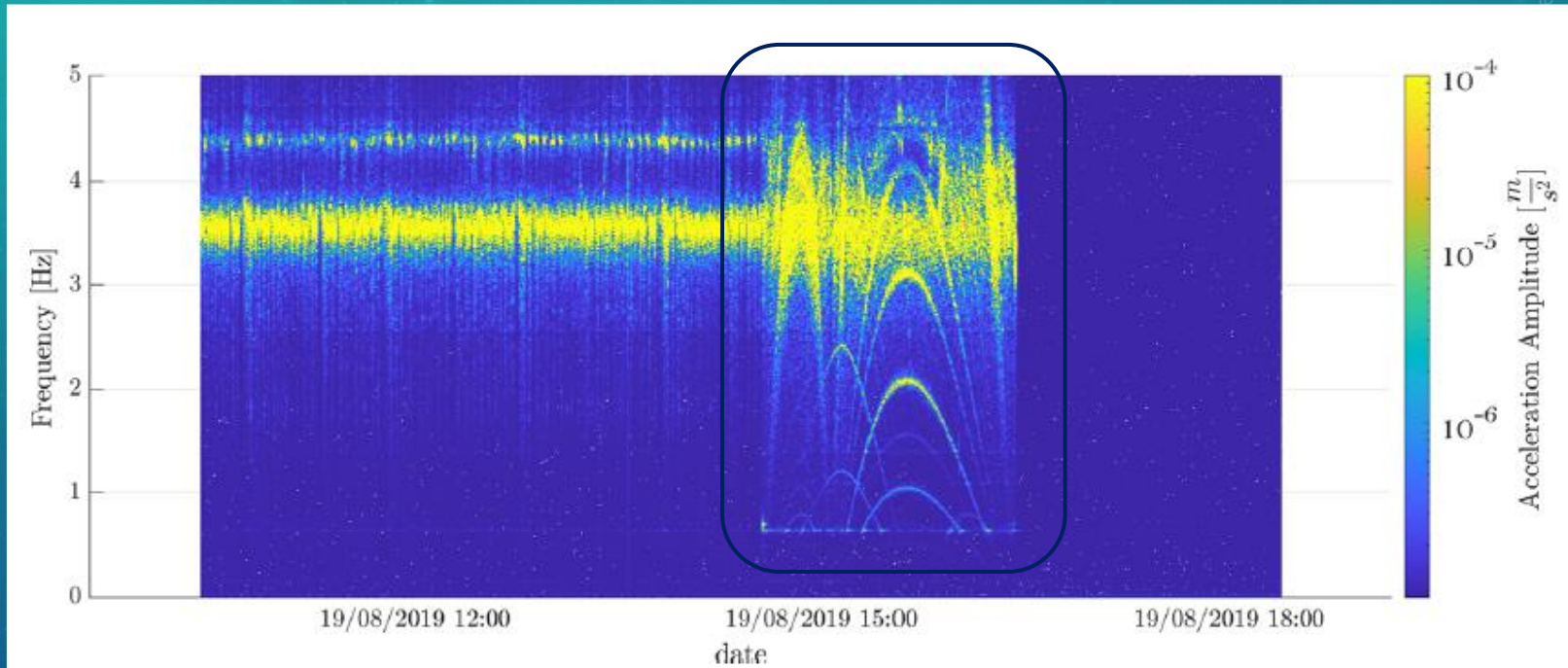
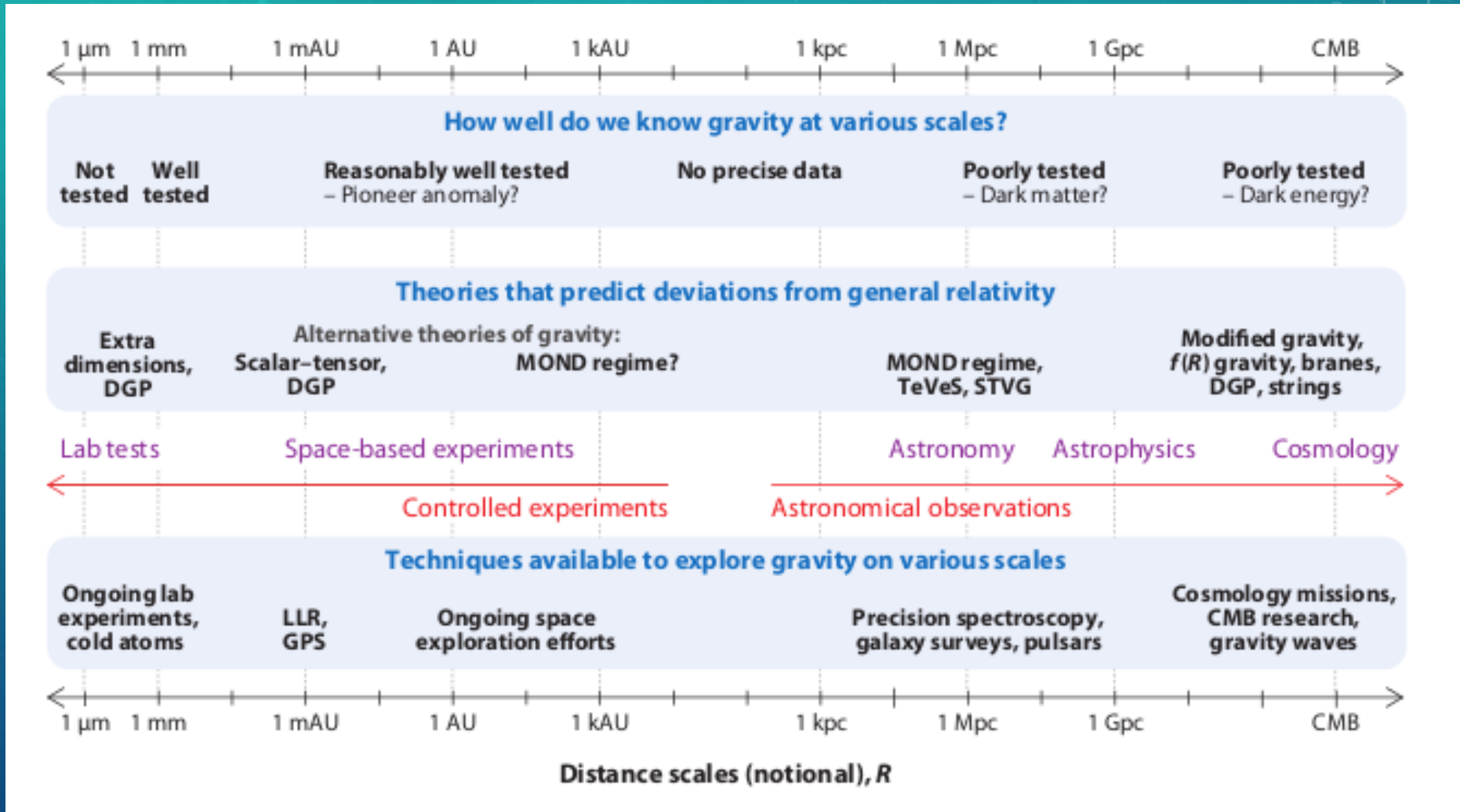


Fig. 14 ISA spectrogram for accelerometer 1 (ISA Y) on 19 August 2019, from 10:25:00 to 18:25:00. Note the signatures of the four reaction wheels from 14:35:00 to 16:27:00

BepiColombo ISA Science Team, Santoli+ 2020



WIDENING THE SIGHT...



The background is a blue gradient with faint technical diagrams and circular patterns. On the right side, there are several circular diagrams with concentric lines and arrows, resembling a gauge or a circular scale. The numbers 100, 110, 120, 130, 140, 150, 160, 170, 180, 190, and 200 are visible on one of these diagrams. There are also dashed lines and arrows indicating movement or flow. The overall aesthetic is clean and modern, with a focus on technical or scientific themes.

Thank you for
your attention